Design and Implementation of a Tunable, Duffing-Like Electronic Resonator via Nonlinear Feedback

Nikhil Bajaj, Andrew B. Sabater, Jeffrey N. Hickey, George T.-C. Chiu, and Jeffrey F. (Jeff) Rhoads

***Abstract*— To date, many vibration-based sensing modalities have relied upon monitoring small shifts in the natural frequency of a system to detect structural changes (e.g., in mass or stiffness), which are attributable to the chemical or biological species, or other phenomena, that are being measured. Often, this approach carries significant signal processing expense due to the presence of electronics, such as precision phase-locked loops, when high sensitivities are required. Bifurcation-based sensing modalities, in contrast, can produce large easy to detect changes in response amplitude with high sensitivity to structural change if applied appropriately. This paper demonstrates the design and implementation of a tunable, Duffing-like electronic resonator realized via nonlinear feedback electronics, which uses a quartz crystal tuning fork as the device platform. The system in this manifestation uses collocated sensing and actuation, along with readily available electronic components, to realize the desired behavior. The sensitivity of the device is tunable via the control of feedback gain and the type of Duffing-like response (hardening or softening) is also selectable, thus creating a versatile bifurcation-based sensing platform. [2015-0014]**

***Index Terms*— Nonlinear circuits, bifurcation, tunable circuits and devices, microsensors.**

I. Introduction

MICROELECTROMECHANICAL systems (MEMS) based sensing is an important area of transducer development and has been so for the past several decades. This importance stems from its potential to provide low-cost, scalable, and sensitive sensor alternatives based upon a wide variety of modalities. Resonant mode sensing is common in MEMS devices and is founded on correlating changes in the resonant behavior of structures and devices to identifiable parameter changes. Traditional methods in this area rely on linear or pseudo-linear sensing, which, in turn, rely on a shift in the resonant frequencies of a vibrating structure to detect changes, either in the device structure or its surroundings. These methods have been successfully used to detect a number of chemical species and other small masses (picograms and smaller in many cases) [1]–[4], and have also found use in applications such as atomic force microscopy (AFM) [5]. It is important to note that performing sensing in the linear mode with high sensitivity requires careful system design and may require significant cost or complexity to implement. It may require phase-locked loops, lock-in amplifiers, or other specialized equipment to perform the measurements and yield high sensitivity in frequency shift measurement.

Bifurcation-based mass sensing, on the other hand, is an approach to mass sensing that relies upon nonlinear behavior to produce large changes in amplitude when a mass change threshold is exceeded. Previous successful sensing efforts using bifurcation-based sensing have achieved high sensitivity [6], [7] albeit with the tradeoff being that the methods usually do not measure mass in a quantifiable manner aside from a certain threshold being exceeded. Taking advantage of nonlinear behavior in similar dynamic systems to increase sensitivity is an active research area [8] and provides additional motivation for the development of devices that exhibit exploitable bifurcation behavior.

Many microscale resonator devices capable of operating in a nonlinear regime commonly exhibit classical Duffing-like frequency responses. These devices can exhibit multiple coexisting steady-state solutions (stable and unstable), saddle-node bifurcations, and hysteretic behavior [9]. A potential disadvantage to the state of the art in bifurcation-based sensing in microscale devices is the fact that in many cases the systems must be driven with magnitudes of excitation that may damage the device (in [6], 18 V peak-to-peak excitation was required, even though the device has a nominal breakdown voltage of 10 V). It is possible to compensate for this by redesigning devices specifically for bifurcation-based sensing [10], but this may not be economical or practical for all applications. Higher drive amplitudes require higher power circuitry to function, reducing applicability for battery powered, low power, mobile sensing.

One approach to tackling the aforementioned issue is to use feedback to produce a bifurcation at lower drive amplitudes. Prior work in this area [11] has used a bistable system structure rather than that of a Duffing resonator, but also had the disadvantage of the vibration actuation being separate (non-collocated). Nonlinear feedback methods have been suggested for use in MEMS devices in the past, generally for the reduction or elimination of nonlinear behavior [12]–[14], but also for improving performance and widening operating regions. The majority of these efforts

Manuscript received January 15, 2015; revised July 18, 2015; accepted October 5, 2015. Date of publication November 3, 2015; date of current version February 1, 2016. This work was supported by the U.S. Department of Homeland Security's Science and Technology Directorate, Office of University Programs, under Award 2013-ST-061-ED0001. Subject Editor A. M. Shkel.

The authors are with the School of Mechanical Engineering, Ray W. Herrick Laboratories, and the Birck Nanotechnology Center, Purdue University, West Lafayette, IN 47907 USA (e-mail: bajajn@purdue.edu; andrew.sabater@gmail.com; hickey1@purdue.edu; gchiu@purdue.edu; jfrhoads@purdue.edu).

Color versions of one or more of the figures in this paper are available online at http://ieeexplore.ieee.org.

Digital Object Identifier 10.1109/JMEMS.2015.2493447

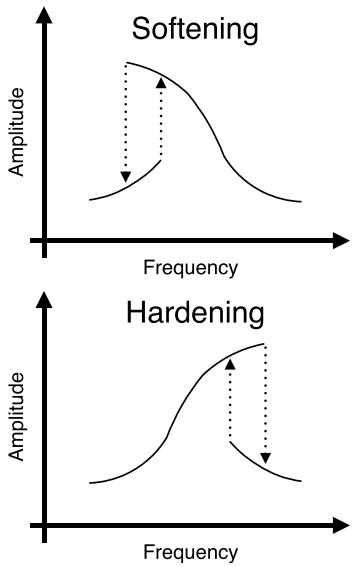

Fig. 1. Examples of softening- and hardening-type Duffing resonator magnitude-frequency response curves.

have been performed either in simulation or on relatively low-frequency, macro-scale analogs of MEMS systems.

The present work demonstrates a method for producing a tunable bifurcation in a system that would otherwise be well characterized with a linear model. The bifurcation used is that which arises in the frequency response of Duffing resonators, namely a saddle-node or cyclic-fold. In this manuscript a low cost device (quartz crystal tuning fork resonator) is used as the platform for demonstration. This device has the advantage of being a piezoelectric device, and thus, collocated actuation and sensing of the vibrational behavior is possible and relatively straightforward to achieve [15]. The selected device presents challenges due to the relatively high-frequency of operation required to implement a nonlinear feedback loop, and the fact that standard digital control methods have significant disadvantages at such frequencies, especially from implementation cost and phase-lag perspectives. To show practical implementation on a class of devices that operates at the high frequencies typical of many MEMS devices, an analog feedback loop consisting of operational amplifiers, passive components, and multipliers capable of providing the cubic nonlinearity used to produce the bifurcation behavior with minimal phase lag are employed. Finally, the sensitivity and bifurcation points of the device are shown to be tunable via control of the feedback gain and the overall excitation amplitude. The type of Duffing-like response (hardening or softening) is made selectable, allowing for a versatile platform suitable for Duffing-like bifurcation-based sensors.

II. Design Concept

A. Sensing Strategy

Bifurcation-based mass sensing relies upon nonlinear behavior to produce large changes in amplitude when a mass change threshold is exceeded. Duffing resonators have a characteristic frequency response which qualitatively depends on whether

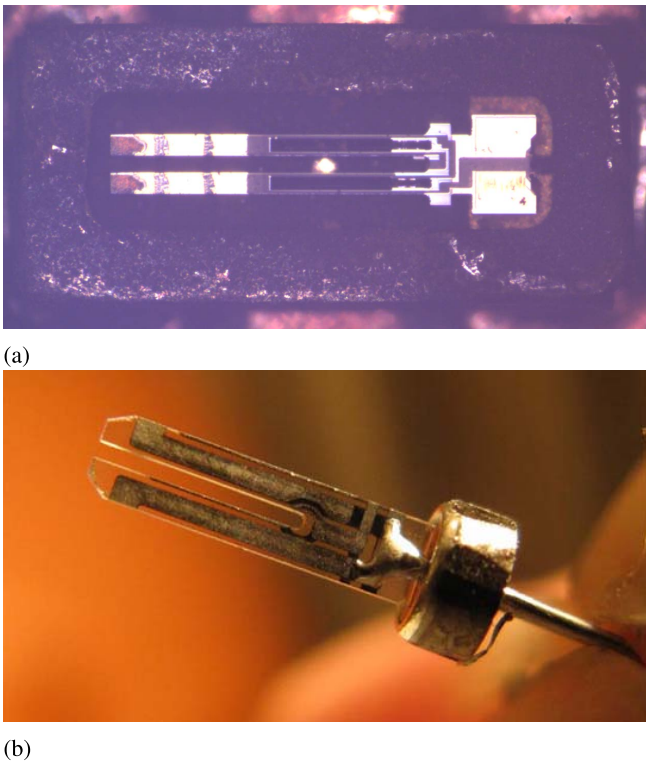

(a)

(b)

Fig. 2. Examples of quartz tuning fork devices: (a) Epson FC-135, (b) Abracon AB38T.

the resonator is hardening or softening as shown in Figure 1. When performing a frequency sweep on a softening-type Duffing resonator, when the frequency is increasing, the system follows one trajectory until the bifurcation frequency, and then it jumps to the other stable trajectory. This occurs when the frequency is decreased as well, but the jump frequencies are different for the increasing and decreasing cases. If the excitation frequency is just below the bifurcation frequency, and the mass of the device increases, the bifurcation frequency decreases, and if it passes the excitation frequency, a jump event will occur. This is the premise of the sensing method.

B. Theory of Operation

The softening Duffing resonator is an ideal model to approximate the dynamics of a real system suitable for sensing. In the present implementation, the demonstration device is a quartz tuning fork, a class of devices that is well-studied due to its use in timing, as well as in linear mass sensing and AFM applications. They are low cost due to being mass-produced, and have relatively tight tolerances and repeatability in a number of aspects of their fabrication. Two examples of quartz tuning fork devices are shown in Figure 2.

As discussed in [16], a common model for a quartz tuning fork is the Butterworth-Van Dyke model (Figure 3), which is an electrical model that incorporates a motional branch representing the piezoelectric behavior (corresponding to the mechanical behavior and comprised of in-series resistance, capacitance, and inductance) in parallel with a purely capacitive branch that represents the capacitance of the device itself.

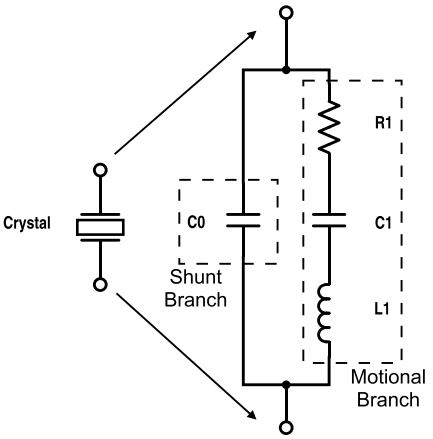

Fig. 3. Classical Butterworth-Van Dyke model of a quartz crystal, applicable for tuning forks and other crystal configurations.

The mechanical behavior can be described by

$$M\ddot{x} + h\dot{x} + kx = F(t). \tag{1}$$

Here, h is an equivalent damping term, M is an equivalent mass term, k is an equivalent stiffness term, x is the displacement (mechanical), and $F(t)$ is the forcing term. In the Butterworth-Van Dyke model the electrical charge stored in the device, q, is divided between the shunt capacitance and the motional capacitance, and the charge in the motional capacitance is proportional to the displacement x. Around resonance one can assume that the motional branch is dominant, which results in a very simple second-order (linear) harmonic resonator model as a first approximation. It should be noted that including a shunt capacitance would model the antiresonance effect common to these devices, and that even better models exist for some quartz tuning fork devices [17]. However, more specific models are not applicable to a wide variety crystal devices, because they differ in geometry and boundary conditions. The approximate model presented here should roughly apply to many devices, not just the tuning forks. For example, the Butterworth-Van Dyke model is used in modeling the transducers used in quartz-crystal microbalances (QCMs) [18]. Finally, it should also be noted that the linear Butterworth-Van Dyke model is used for devices in their normal operating voltage and current ranges, which is where the nonlinear circuit will operate as well. This alleviates concerns about device reliability and longevity.

In order for the device to behave as a Duffing-type system, a cubic nonlinearity needs to be introduced. This nonlinearity can be added to the system via feedback, since $F(t)$ is prescribed externally. If $F(t)$ is chosen such that

$$F = F^*(t) - \alpha x^3, \tag{2}$$

then the resulting system equation becomes:

$$M\ddot{x} + h\dot{x} + kx + \alpha x^3 = F^*(t). \tag{3}$$

In this case, $F^*(t)$ will be a sinusoidal input $A\sin(\omega t)$. The Duffing response can now be tuned by controlling the feedback gain α.

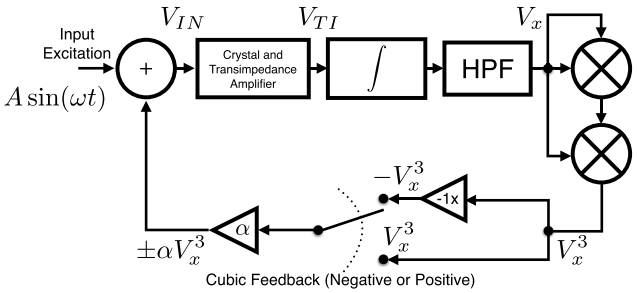

Fig. 4. Schematic representation of the design concept.

In order to measure the effective position of the sensor, x, the piezoelectric nature of the device can be exploited. The piezoelectric characteristics of the quartz material can also be used to simultaneously provide the excitation to the device. Thus, the device can be driven by a summing amplifier that adds an input excitation $V_{IN}(t)$ with the desired cubic feedback. The drive amplifier will excite the crystal through a transimpedance circuit with high gain, to produce a voltage proportional to the current passing through the crystal due to the drive input. This voltage, V_{TI}, is therefore proportional to $\dot{x}$. To produce a voltage proportional to x, V_{TI} is integrated, then passed through a high-pass filter (HPF) to eliminate DC offset. Following the filtering, the output V_x is proportional to x, and the quantity is passed through two analog multipliers in order to create a value proportional to x^3. This is passed through an inverter, and either the inverted cubed signal or the original cubed signal is passed through a non-inverting gain amplifier to produce a voltage proportional to αx^3 which is then summed into the input excitation to complete the feedback loop. The design schematic can be seen in Figure 4.

Theoretically, the method detailed above should be applicable as either an analog or digital implementation. However, such resonator systems and their nonlinear behavior are generally phase-sensitive [13]. For slower systems (in terms of natural frequency and bifurcation frequencies) digital design may be practical. However, for the crystals used in this platform, with a resonant frequency close to 32.760 kHz, sampling at the "rule-of-thumb" of 20 times the nominal control frequency for feedback control applications would introduce a phase lag of approximately 18 degrees. This would likely not allow desired results. This would also require a digital control loop operating at >600 kHz, which is achievable but difficult. Sampling at 100 times the frequency would introduce 3.6 degrees of phase lag, assuming that the output can be produced within one sampling period, but would require a digital control loop operating at >5 MHz, and would require significant cost and design effort. In addition, without careful smoothing and filtering, DAC outputs may introduce quantization noise that may cause premature bifurcation. Therefore, from the perspective of design practicality, cost, and performance, an analog solution was selected.

C. Design Guidelines

The circuit consists of three main subsystems: the actuation and sensing subsystem, the filtering subsystem, and the cubic

feedback generation subsystem. Frequency ranges and excitation voltage ranges of interest will depend on the device used as the sensing platform. As an example, most commercially available quartz tuning forks range in operating frequency from 10 kHz to 200 kHz, while other quartz resonators can operate up to the hundreds of MHz or higher range (using overtones, and not in tuning fork geometries). Voltage ranges of operation span from less than one volt to tens of volts. While the methodology used to produce the bifurcation is applicable to a wide range of devices as long as one has direct control over the sensing and actuation circuitry, only the design guidelines for working with piezoelectric, collocated sensing and actuation devices are discussed here.

1) Sensing and Actuation Subsystem: Collocated sensing and actuation is a well-studied area in structural mechanics and control, and in particular has been very carefully studied in the area of AFM and scanning probe microscopy (SPM) systems, where quartz tuning forks are commonly used as actuation and sensing elements. One common method of simultaneously driving and sensing the behavior of a piezoelectric device is that of driving it through a bridge circuit [19]–[21], which is either active or passive. As with most bridge circuits, tuning is generally required after construction in order to get the best performance out of the circuit, due to tolerances and parasitic capacitance and inductance. The key advantage of the active bridge circuit is to remove the asymmetry present in the frequency response that arises from the shunt capacitance, as seen in the commonly-used Butterworth-Van Dyke model [15], along with providing high sensitivity and low noise. However, low noise and high sensing gain can be achieved without the use of shunt capacitance compensation, if one is willing to accept the asymmetry in the response. In this work, a simple transimpedance amplifier configuration is used.

In order to design the transimpedance amplifier stage it is important to characterize the equivalent series resistance (ESR) of the device. The ESR is the equivalent impedance of the crystal resonator measured at the electrical resonant frequency. Based on the ESR (provided by the manufacturer or determined via impedance measurement), the approximate current consumption of the device [root-mean squared (RMS) should be sufficient for this purpose] can be estimated for a given input voltage magnitude. The maximum current consumption should occur near electrical resonance. In order to provide a useful signal-to-noise ratio for later stages, a transimpedance gain (feedback resistor) can be chosen such that the voltage output of the transimpedance stage uses a reasonable fraction (10% or more) of the dynamic range. Photodiode measurement transimpedance circuits deal with a similar range of currents and design considerations for them are widely available [22] – the same guidelines apply here, with low input bias and input offset current being key design parameters. The output of the transimpedance stage should drive the filtering subsystem.

2) Filtering Subsystem: As discussed previously, the filtering subsystem consists of an integrator and a high-pass filter circuit. The integrator should have sufficiently wide bandwidth for the system, with minimal distortion and the useful integration frequency range spanning at least a decade below the operating frequency and allowing attenuated integration of the third harmonic. Integrator design is a standard operational amplifier design technique, as is high-pass filter design [23]. The design should use an operational amplifier with a low input offset voltage but sufficient bandwidth to meet requirements.

3) Nonlinear Feedback Subsystem: The nonlinear feedback subsystem consists of gain and/or attenuation circuits, the circuitry to produce the cubic signal, and finally the summing amplifier which adds together the excitation and the nonlinear feedback. Gain and attenuation circuits can be created using standard operational amplifier designs, with adjustable gains useful for tuning the bifurcation response. Adjustable gain and attenuation can be conveniently built into the circuit through the use of potentiometers, or alternatively, through additional multiplier elements, variable gain amplifiers (VGAs) or programmable gain amplifiers (PGAs). The option of adding a gain or attenuating intermediate signals allows one to constrain the input ranges of the subsequent elements to avoid saturation while maximizing dynamic range. One method of doing this is to drive the tuning fork to resonance with a desired drive amplitude input excitation (a frequency sweep may be required to find it) and then observe intermediate signals, tuning them such that they do not saturate but take up a significant fraction of the dynamic range of the amplifiers and multipliers.

The drive amplifier chosen should be able to drive highly capacitive loads in a stable manner. Many operational amplifiers have maximum capacitive loading for stable operation provided in their specifications data, and this should be compared to the measured impedance of the device being driven. The drive amplifier is configured as a summing amplifier to add together the input excitation signal and the cubic feedback signal, which should have some option of attenuation/gain control in order to tune the feedback gain.

In general, following best practice low-noise, precision analog circuit design is recommended, including designing the circuit to reduce stray capacitance and appropriately shielding cables [24].

III. Implementation

The utilized drive/summing amplifier is a LM7321 from Texas Instruments due to its specification for driving reactive and capacitive loads and sufficient bandwidth, and the transimpedance amplifier is a THS4601 from Texas Instruments, a very high speed FET-input amplifier, chosen due to its low input bias current and high bandwidth, which allows for a sufficient bandwidth at the operating frequency while having a high transimpedance gain of 2 MΩ. The integrator stage uses an OPA37 (also from Texas Instruments), all subsequent operational amplifiers used (in the high-pass filter and for buffer amplifiers for observing signals) are OPA192 low-noise precision amplifiers from Texas Instruments (they have sufficient bandwidth for the tasks) and the utilized multipliers are AD633 (from Analog Devices) devices. The electronics were laid out on a printed circuit board (PCB) with multiple diagnostic outputs for observation with an oscilloscope, including the transimpedance amplifier output, the integrator and high-pass filter output, the squared output, and the cubic

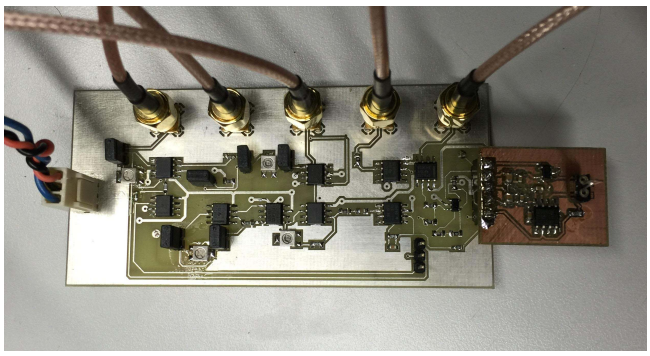

Fig. 5. Implementation of the design. The tuning fork can be seen still in its package on the smaller PCB (on the right), along with the drive and transimpedance amplifiers.

output. Potentiometers and non-inverting amplifiers control the feedback gains and gains between multiplier stages, and $0.1''$ pitch header jumpers are used to allow the potentiometer values to be measured to determine the gain at the individual amplification stages. In addition, a jumper allows selection of positive, negative, or no cubic feedback into the summing amplifier. The implementation is shown in Figure 5, with the detailed circuit diagram shown in Figure 6. The experiment is provided power from a standard lab dual voltage power supply supplying $+15$V, -15V, and ground. The input excitation signal is provided using an Agilent 55321 waveform generator, and the output measurements are taken on a Agilent MSO-3104A 4-channel oscilloscope. Both the waveform generator and the oscilloscope are connected to a host PC utilizing USB, and they are correspondingly controlled via a LabVIEW script and drivers provided by National Instruments and Agilent. The desired frequency response structure was produced by tuning the feedback potentiometers, starting at the lowest gain values, and then slowing increasing them while sweeping the frequency of the signal driving the device.

This particular system implementation has the transimpedance board isolated from the analog signal processing board, in order to facilitate the use of multiple types of devices for measurement (the measured device is mounted to the transimpedance amplifier board along with the drive amplifier to minimize trace length and therefore parasitic inductance, capacitance, and impedance while driving the crystal). Certain through-hole crystals (for example, Abracon Corporation Model AB38T) and surface mount crystals (for example, Epson FC-135) are supported, depending on the footprint.

Behavior is characterized by performing frequency sweeps of the input excitation. The output waveform (the integrator output, representing x, is measured on the oscilloscope, and the frequency, input excitation magnitude, and output excitation magnitude are all measured using the oscilloscope with averaging of 16 waveforms, in addition to adaptively switching the scale of the oscilloscope at each reading in order to maximize resolution. Nominally, the bifurcation frequency is in the 32.700-32.800 kHz range, so a coarse sweep is initially performed with frequency steps of 2 Hz. After a bifurcation is localized, the frequency steps around that point are made more fine (0.1 Hz) and the frequency range over which measurements are taken is tightened in order to speed up the measurements. A dwell time of 3 seconds per measurement was used in these experiments in order to allow the system to reach a steady state after each frequency change. The sweeps are performed both increasing and decreasing in order to appropriately characterize hysteresis. In addition, in a number of the tests, the magnitudes were changed between sweeps in order to determine the effect of input excitation magnitude. Feedback gain was also varied in some of the tests.

It is important to note that to reproduce results consistently, the frequency step sizes should be consistent, as a frequency jump as produced by the signal generator near the bifurcation, if too large, may cause a bifurcation jump event to the other branch. A larger frequency jump will cause the system to jump more easily. As discussed earlier, for this work, the frequency step was 0.1 Hz around the bifurcation point, but depending on the sensitivity of the device a lower or higher step size may be appropriate. It is also important to make certain that the function or signal generator used to generate the excitation input operates in a phase-continuous manner when changing frequency, as non-phase-continuous behavior can very briefly introduce broad spectrum excitation, which can cause a bifurcation event as well. In general, noise can cause the system to jump unexpectedly as well, so noise-reduction practices such as ground planes, shielded/coaxial cabling, and relatively clean power supplies should be used. The amount of noise that can be tolerated is device and application dependent, and related to the desired sensitivity of the bifurcation and the frequency resolution of excitation and measurement equipment.

IV. Results and Discussion

The following results were generated using an Abracon Corporation model AB38T tuning fork crystal designed for clock circuits operating at 32.768 kHz. The proof-of-concept results are discussed here.

A. Generation of Bifurcations and Tunability

In order to demonstrate the tunability of the response, the input excitation magnitude was held constant at 75 mV peak-to-peak. The feedback jumper was also left unconnected initially so that there would be no feedback contribution to the input excitation. Thus, the expected response in this case would be a linear one. Then the system was connected to negative feedback, and the system was characterized with two values of the feedback gain. Following this, the system was switched to positive feedback, and the system was characterized again with multiple values of the feedback gain. The results are plotted in Figure 7 and demonstrate the ability of this approach to produce a bifurcation that can be tuned based on system requirements by modifying the feedback gain. In all of the experimental results, the tuning forks have a portion of the housing removed to expose them to air. While this increases effects associated with dissipation, it is a more realistic system for use as a bifurcation-based sensor. For all of the frequency response plots in this paper, the data points represent the peak-to-peak magnitude of the response signal, with

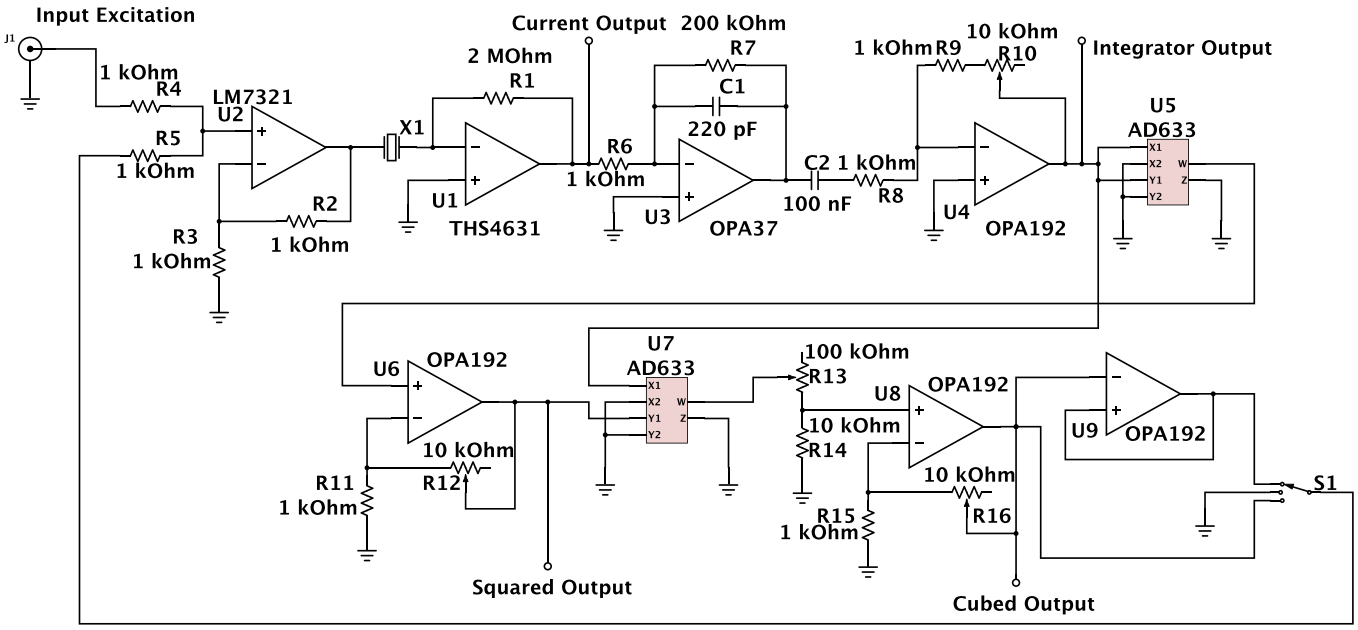

Fig. 6. Detailed circuit diagram. Note that power supply lines are omitted aside from ground, as are buffer operational amplifiers from the output connections, and decoupling capacitors.

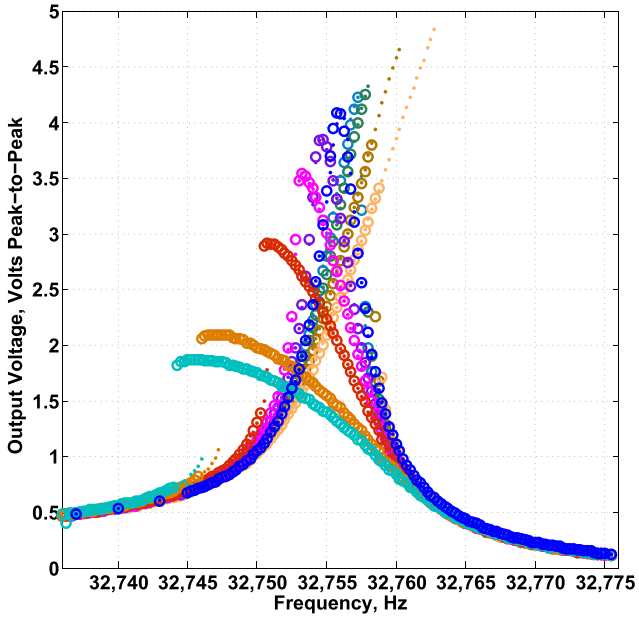

Fig. 7. Demonstration of the tuning of the Duffing-like bifurcation response, with both hardening and softening characteristics. The applied excitation is a sine waveform with magnitude of 75 mV peak-to-peak.

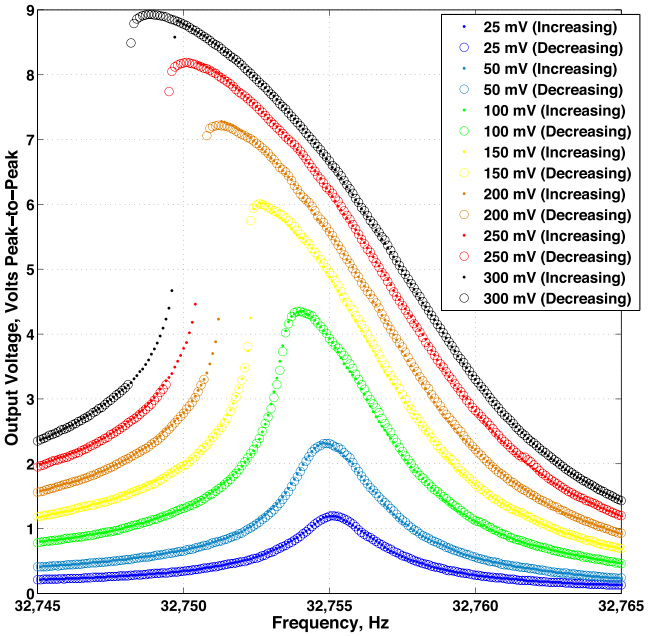

Fig. 8. Demonstration of the tuning of the Duffing-like frequency response in the softening feedback mode, with a fixed gain and varying excitation amplitude.

dots representing data acquired during sweeps with increasing frequency, and the circles representing data acquired during sweeps with decreasing frequency. Repeatability experiments were performed by using three different AB38T tuning forks (again, removed from the housing) and then performing a linear response characterization (discrete frequency sweep) with fixed 75 mV peak-to-peak input excitation. The nonlinear feedback was then connected to the circuit with the same input excitation magnitude, and the same feedback gain (softening) for each device. Trials with three devices are shown in Figure 10. The effect is repeatable with the same gains for the same devices producing a similar (though not identical) response. The responses could be made closer by tuning the gains further to match and compensate for device-to-device variation.

B. Response at Varying Input Magnitudes

To further demonstrate the Duffing-like behavior of the system, the feedback gain was held fixed for both a softening

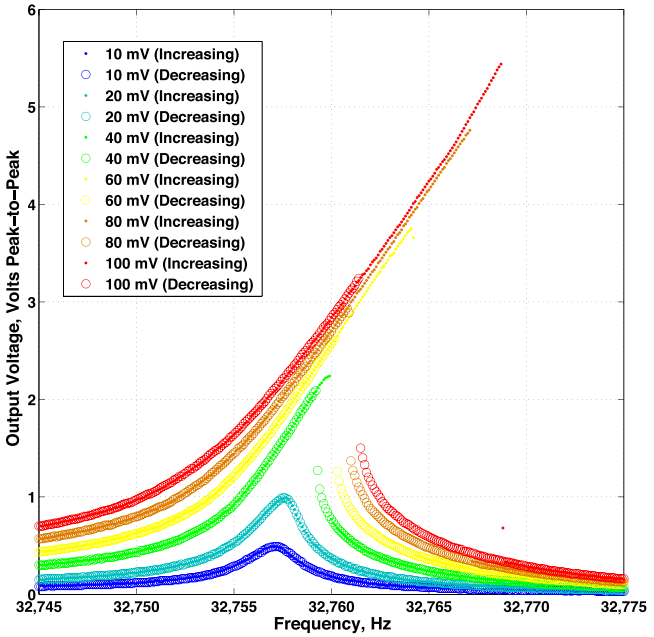

Fig. 9. Demonstration of the tuning of the Duffing-like frequency response in the hardening feedback mode, with fixed gain and varying excitation amplitude.

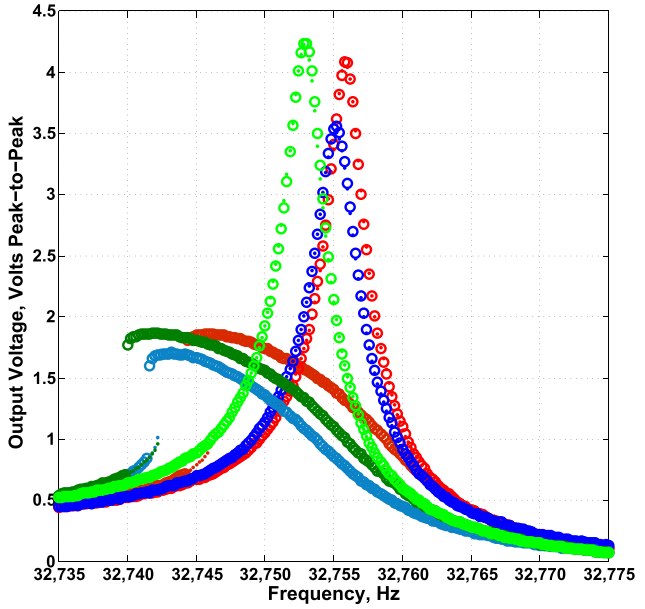

Fig. 10. Softening responses of three different AB38T tuning fork crystal devices, with their respective linear responses shown as well. These devices were excited with the same fixed feedback gain (for the softening case) and the same input excitation.

case (Figure 8) and a hardening case (Figure 9). In each case, the input excitation magnitude was increased between frequency sweeps, and the amplitude-dependent response typical of Duffing resonator systems [25] is clearly present. In the case of the softening case, in order to have a bifurcation, it is clear that for this particular gain (set by the potentiometer) the system requires a minimum excitation amplitude of approximately 150 mV peak-to-peak. Similarly, the minimum excitation amplitude required for bifurcation in the hardening response for this particular gain is approximately 40 mV peak-to-peak. Both of these values are generally within safe operational ranges for the device.

C. Applicability to Multiple Crystal Types

After demonstrating the method successfully with Abracon Corporation AB38T devices, an attempt was made to determine applicability to other devices using the same circuit. An Epson FC-135 device was soldered to the transimpedance amplifier board in the appropriate footprint and was subjected to a softening-mode feedback with varying input amplitude, and the results, shown in Figure 11, indicate that the method is likely adaptable and applicable to a range of devices. Comparing the two devices, the FC-135 is approximately 1/2 to 1/3 the size of the AB38T tuning fork, with significant difference in the aspect ratio of tine length to tine thickness, required to maintain the same operating frequency. The electrode configuration and tine shape also have some significant differences in design. The equivalent series resistance is also higher in the FC-135 devices (approximately 80 kΩ as compared to approximately 40 kΩ). Despite the differences, the devices behave similarly enough to allow the bifurcation response to be created on the FC-135 as well, with some tuning of feedback and internal

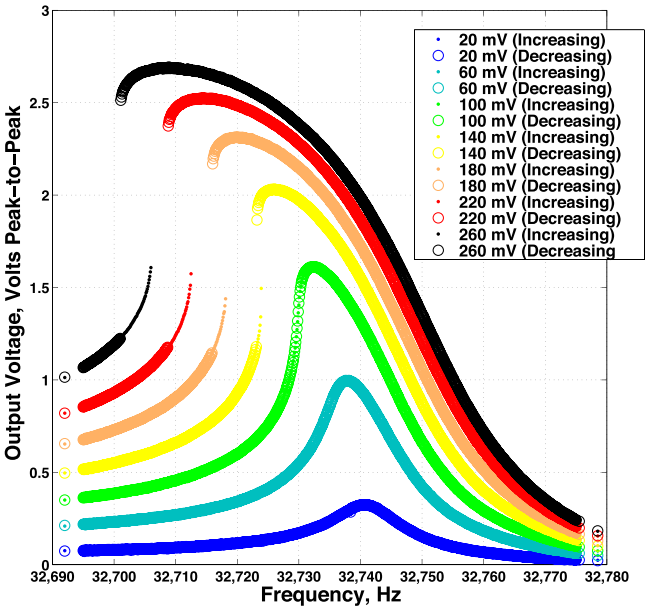

Fig. 11. Demonstration of tuning of Duffing-like frequency response in the softening mode for the Epson FC-135 tuning fork crystal, with a fixed gain and varying excitation amplitude.

multiplier and filter gains. It should be noted that the softening mode behavior (Figures 8 and 11) experimental results show additional softening near the bifurcation frequency that is not typical of a nonlinear oscillator with quadratic and/or cubic nonlinearities [25]. These may arise from unmodeled dynamics in the form of additional nonlinear damping terms. In particular, it is hypothesized that the atypical behavior may be explained as resulting from the shunt capacitor in the Butterworth-Van Dyke model and the nonlinear damping that it contributes when the measured current is passed through the cubic feedback. This is an area of future investigation.

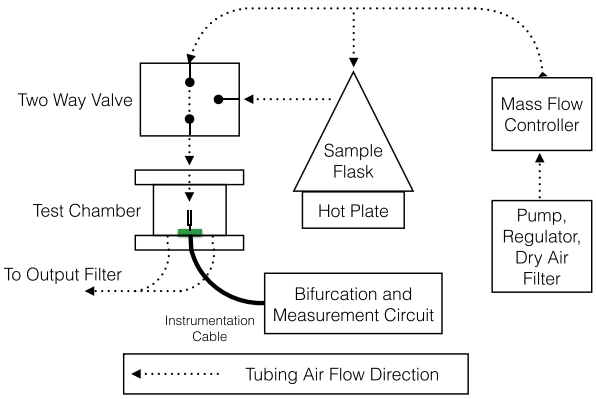

Fig. 12. Water vapor detection test configuration.

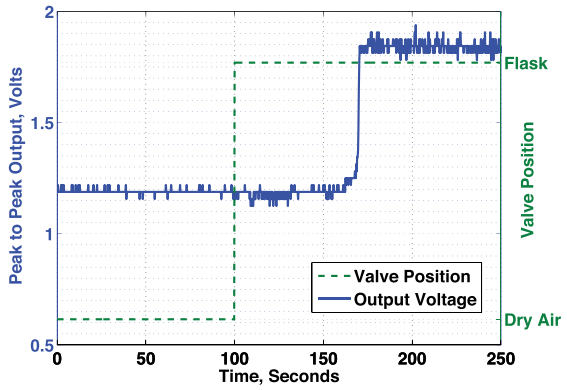

Fig. 13. Water vapor detection test.

D. Sensor Test

As a preliminary sensing experiment, an apparatus was developed to test the behavior of the device when exposed to an increase in humidity, which would add a small amount of condensation onto the device (and also likely increase damping). The system was comprised of a test chamber containing an Epson FC-135-based sensor, a mass flow controller (MFC), a two-position valve, and a flask that contained boiling water atop a hot plate. A diaphragm pump was used to provide sufficient pressure for the operation of the MFC. This is shown in Figure 12. The device was configured for a softening bifurcation and allowed to reach steady state at an excitation frequency 0.3 Hz below the bifurcation frequency. At a certain time, the valve supplying air to the test chamber was switched from dry air to air from the flask. The resulting response is shown in Figure 13. This indicates the bifurcation of the device behavior in response to the humidity increase. The time delay is related to the relatively large volume of the device chamber (approximately 150 cm^3) in comparison to the flow rate (50 mL/min).

V. Conclusions

A system and circuit design was presented that creates a Duffing-like resonator system using off-the-shelf, relatively low-cost components and creates an opportunity for the low-cost implementation of bifurcation-based sensors. The recovered bifurcations are tunable, and are repeatable on a device to device basis for multiple types of quartz crystal resonator. As another advantage of this method, the required input excitation required is significantly lower than much of the prior art when producing the bifurcation behavior. Future work will focus on understanding the deviations from the ideal Duffing resonator behavior that are present in the experimental platform, as well as the integration of more advanced sensing and control schemes to take advantage of this platform in improving sensor performance, repeatability, and sensitivity.

References

[1] T. Thundat, E. A. Wachter, S. L. Sharp, and R. J. Warmack, "Detection of mercury vapor using resonating microcantilevers," *Appl. Phys. Lett.*, vol. 66, no. 13, pp. 1695–1697, 1995.

[2] M. Villarroya *et al.*, "Cantilever based MEMS for multiple mass sensing," in *Proc. PhD Res. Microelectron. Electron.*, vol. 1. 2005, pp. 197–200.

[3] R. Raiteri, M. Grattarola, and R. Berger, "Micromechanics senses biomolecules," *Mater. Today*, vol. 5, no. 1, pp. 22–29, 2002.

[4] F. M. Battiston *et al.*, "A chemical sensor based on a microfabricated cantilever array with simultaneous resonance-frequency and bending readout," *Sens. Actuators B, Chem.*, vol. 77, nos. 1–2, pp. 122–131, 2001.

[5] A. Raman, J. Melcher, and R. Tung, "Cantilever dynamics in atomic force microscopy," *Nano Today*, vol. 3, nos. 1–2, pp. 20–27, 2008.

[6] V. Kumar *et al.*, "Bifurcation-based mass sensing using piezoelectrically-actuated microcantilevers," *Appl. Phys. Lett.*, vol. 98, no. 15, p. 153510, 2011.

[7] V. Kumar, Y. Yang, J. W. Boley, G. T.-C. Chiu, and J. F. Rhoads, "Modeling, analysis, and experimental validation of a bifurcation-based microsensor," *J. Microelectromech. Syst.*, vol. 21, no. 3, pp. 549–558, Jun. 2012.

[8] C. B. Burgner, W. S. Snyders, and K. L. Turner, "Control of MEMS on the edge of instability," in *Proc. 16th Int. Solid-State Sens., Actuators, Microsyst. Conf. (TRANSDUCERS)*, Jun. 2011, pp. 1990–1993.

[9] J. F. Rhoads, S. W. Shaw, and K. L. Turner, "Nonlinear dynamics and its applications in micro- and nanoresonators," *J. Dyn. Syst., Meas., Control*, vol. 132, no. 3, p. 034001, 2010.

[10] R. L. Harne and K. W. Wang, "A bifurcation-based coupled linear-bistable system for microscale mass sensing," *J. Sound Vibrat.*, vol. 333, no. 8, pp. 2241–2252, 2014.

[11] R. L. Harne and K. W. Wang, "Robust sensing methodology for detecting change with bistable circuitry dynamics tailoring," *Appl. Phys. Lett.*, vol. 102, no. 20, p. 203506, 2013.

[12] D. H. Maithripala, J. M. Berg, and W. P. Dayawansa, "Control of an electrostatic microelectromechanical system using static and dynamic output feedback," *J. Dyn. Syst., Meas., Control*, vol. 127, no. 3, pp. 443–450, 2004.

[13] R. M. C. Mestrom, R. H. B. Fey, and H. Nijmeijer, "On phase feedback for nonlinear MEMS resonators," in *Proc. IEEE Int. Freq. Control Symp.*, May/Jun. 2007, pp. 765–770.

[14] R. M. C. Mestrom, R. H. B. Fey, and H. Nijmeijer, "Phase feedback for nonlinear MEM resonators in oscillator circuits," *IEEE/ASME Trans. Mechatronics*, vol. 14, no. 4, pp. 423–433, Aug. 2009.

[15] Y. Qin and R. Reifenberger, "Calibrating a tuning fork for use as a scanning probe microscope force sensor," *Rev. Sci. Instrum.*, vol. 78, no. 6, p. 063704, 2007.

[16] J.-M. Friedt and É. Carry, "Introduction to the quartz tuning fork," *Amer. J. Phys.*, vol. 75, no. 5, pp. 415–422, 2007.

[17] A. Castellanos-Gomez, N. Agrait, and G. Rubio-Bollinger, "Dynamics of quartz tuning fork force sensors used in scanning probe microscopy," *Nanotechnology*, vol. 20, no. 21, p. 215502, 2009.

[18] S. J. Martin, V. E. Granstaff, and G. C. Frye, "Characterization of a quartz crystal microbalance with simultaneous mass and liquid loading," *Anal. Chem.*, vol. 63, no. 20, pp. 2272–2281, 1991.

[19] J. J. Dosch, D. J. Inman, and E. Garcia, "A self-sensing piezoelectric actuator for collocated control," *J. Intell. Mater. Syst. Struct.*, vol. 3, no. 1, pp. 166–185, 1992.

[20] G. E. Simmers, Jr., J. R. Hodgkins, D. D. Mascarenas, G. Park, and H. Sohn, "Improved piezoelectric self-sensing actuation," *J. Intell. Mater. Syst. Struct.*, vol. 15, no. 12, pp. 941–953, 2004.

[21] S. Zihajehzadeh, M. Maroufi, M. Shamshirsaz, and A. H. Rezaie, "Self-sensing and quality factor control circuits for piezoelectric millimeter-sized resonant cantilevers," *J. Intell. Mater. Syst. Struct.*, vol. 22, no. 17, pp. 2079–2089, 2011.
[22] X. Ramus, "Transimpedance considerations for high-speed amplifiers," Texas Instrum., Dallas, TX, USA, Appl. Rep. SBOA122, 2009, pp. 1–9.
[23] P. Horowitz and W. Hill, *The Art of Electronics*. Cambridge, U.K.: Cambridge Univ. Press, 1989.
[24] M. Thompson, *Intuitive Analog Circuit Design*. Burlington, VT, USA: Newnes, 2006.
[25] A. H. Nayfeh and D. T. Mook, *Nonlinear Oscillations*. Hoboken, NJ, USA: Wiley, 1979.

Nikhil Bajaj received the B.S. and M.S. degrees in mechanical engineering from Purdue University, West Lafayette, IN, in 2008 and 2011, respectively. He is currently pursuing the Ph.D. degree with the School of Mechanical Engineering, Purdue University, West Lafayette. He has held research assistant positions on several projects in the areas of advanced manufacturing, computational design, and heat transfer, and a summer research position with Alcatel-Lucent Bell Laboratories. His research interests include nonlinear dynamical and control systems, and the analysis and design of mechatronic systems.

Andrew B. Sabater received the B.S. (Hons.) degree in general engineering from Harvey Mudd College, Claremont, CA, USA, in 2009, and the M.S. and Ph.D. degrees in mechanical engineering from Purdue University, West Lafayette, IN, USA, in 2012 and 2014, respectively. His current research includes the predictive design, testing, and analysis of isolated and coupled resonant microelectromechanical systems, with applications in chemical and biological sensing, electromechanical signal processing, and timing and navigation.

Jeffrey N. Hickey is currently pursuing the B.S. degree in mechanical engineering with Purdue University, West Lafayette, IN. Along with being a student with the Purdue Honors College, he is also pursuing a minor in electrical and computer engineering, and a Certificate in Entrepreneurship. He is an Undergraduate Research Assistant. He has participated in undergraduate research for two semesters, the duration of which he has assisted in various sensing related projects, aided in electronic circuit design and development, and performed system testing and debugging.

George T.-C. Chiu received the B.S. degree from National Taiwan University, in 1985, and the M.S. and Ph.D. degrees from the University of California at Berkeley, in 1990 and 1994, respectively, all in mechanical engineering. He was with Hewlett-Packard, designing printers and multifunction devices. He is currently a Professor with the School of Mechanical Engineering with courtesy appointments in the School of Electrical and Computer Engineering, and the Department of Psychological Sciences, Purdue University. His current research interests are mechatronics, and dynamic systems and control with applications to digital printing and imaging systems, digital fabrications and functional printing, human motor control, and motion and vibration perception and control. He is a Fellow of ASME, and the Society for Imaging Science and Technology. He received the 2012 NSF Director's Collaboration Award, the 2010 IEEE TRANSACTIONS ON CONTROL SYSTEM TECHNOLOGY Outstanding Paper Award, the Purdue University College of Engineering Faculty Engagement/Service Excellence Award in 2010, and the Team Excellence Award in 2006. He was the Chair of the Executive Committee on the ASME Dynamic Systems and Control Division from 2013 to 2014.

Jeffrey F. (Jeff) Rhoads received the B.S., M.S., and Ph.D. degrees from Michigan State University, in 2002, 2004, and 2007, respectively, all in mechanical engineering. He is an Associate Professor with the School of Mechanical Engineering, Purdue University, and is affiliated with both the Birck Nanotechnology Center and Ray W. Herrick Laboratories at Purdue University. His current research interests include the predictive design, analysis, and implementation of resonant micro/nanoelectromechanical systems for use in chemical and biological sensing, electromechanical signal processing, and computing; the dynamics of parametrically-excited systems and coupled oscillators; and the behavior of electromechanical and thermomechanical systems, including energetic materials, operating in rich, and multiphysics environments. He is a Member of the American Society for Engineering Education (ASEE) and the American Society of Mechanical Engineers (ASME), where he serves on the Design, Materials, and Manufacturing Segment Leadership Team, and the Design Engineering Division's Technical Committees on Micro/Nanosystems and Vibration and Sound. He is a recipient of the National Science Foundation's Faculty Early Career Development Award, the Purdue University School of Mechanical Engineering's Harry L. Solberg Best Teacher Award (twice), and the ASEE Mechanics Division's Ferdinand P. Beer and E. Russell Johnston, Jr. Outstanding New Mechanics Educator Award. In 2014, he was selected as the inaugural recipient of the ASME C. D. Mote Jr., Early Career Award and was featured in ASEE Prism Magazine's 20 Under 40.